

Nucleoside conformers in low-temperature argon matrices: Fourier transform IR spectroscopy of isolated thymidine and deuteriothymidine molecules and quantum-mechanical calculations

Cite as: *Low Temp. Phys.* **45**, 1008 (2019); <https://doi.org/10.1063/1.5121271>
 Published Online: 27 September 2019

A. Yu. Ivanov, S. G. Stepanian, V. A. Karachevtsev, and L. Adamowicz



View Online



Export Citation



CrossMark

ARTICLES YOU MAY BE INTERESTED IN

[Plastic Flow of Solid \$^4\text{He}\$ and \$^3\text{He}\$ at Low Temperatures \(Review Article\)](#)

Low Temperature Physics **45**, 964 (2019); <https://doi.org/10.1063/1.5121266>

[Coulomb effects on thermally induced shuttling of spin-polarized electrons](#)

Low Temperature Physics **45**, 1032 (2019); <https://doi.org/10.1063/1.5121274>

[Manifestation of Spin Correlations in Monocrystalline \$\text{ErAl}_3\(\text{BO}_3\)_4\$](#)

Low Temperature Physics **45**, 1041 (2019); <https://doi.org/10.1063/1.5121279>

LOW TEMPERATURE TECHNIQUES
 OPTICAL CAVITY PHYSICS
 MITIGATING THERMAL
 & VIBRATIONAL NOISE

DOWNLOAD THE WHITE PAPER

downloads.montanainstruments.com/optical_cavities

MONTANA INSTRUMENTS
 COLD SCIENCE MADE SIMPLE



Nucleoside conformers in low-temperature argon matrices: Fourier transform IR spectroscopy of isolated thymidine and deuteriothymidine molecules and quantum-mechanical calculations

Cite as: Fiz. Nizk. Temp. **45**, 1181–1191 (September 2019); doi: 10.1063/1.5121271

Submitted: 23 July 2019



View Online



Export Citation



CrossMark

A. Yu. Ivanov,^{1,a)} S. G. Stepanian,¹ V. A. Karachevtsev,¹ and L. Adamowicz²

AFFILIATIONS

¹B. Verkin Institute for Low Temperature Physics and Engineering of the National Academy of Sciences of Ukraine, 47 Nauky Ave., Kharkiv 61103, Ukraine

²University of Arizona, Tucson city 85721, Arizona, USA

^{a)}Email: ivanov@ilt.kharkov.ua

ABSTRACT

The conformational equilibrium of thymidine and deuteriothymidine molecules in low-temperature Ar matrices has been studied using low-temperature matrix-isolation Fourier IR spectroscopy and quantum-chemical calculations by the DFT/B3LYP and MP2 methods. It has been found that two *anti*-conformers ta2_0 and ta3_0 with different structures of the sugar ring, C2'-endo and C3'-endo, predominate in low-temperature matrices. In isolated state, each of these conformers has a few low-barrier satellites that can fully pass into more stable structures when a molecule enters the matrix. The main *syn* conformer ts2_0 is stabilized by an intramolecular hydrogen bond between the O5'H group of the sugar and the C2O group of the base (O5'H...O2), while C2'-endo is the predominant conformation of the deoxyribose ring. The considerably lower population of ts2_0 compared to the *anti*-conformers ta2_0, ta3_0 can be explained by the smaller population of satellite conformations. It has been shown that the absorption band of ν N3D stretching vibration is split by the Fermi resonance.

Published under license by AIP Publishing. <https://doi.org/10.1063/1.5121271>

I. INTRODUCTION

Studies of the structure of constituent fragments of biopolymer molecules in isolated state are of fundamental interest for the contemporary science.^{1–7} For example, such structural elements of DNA and RNA as nucleosides are studied using the most up-to-date high-sensitive spectroscopy methods.^{6,7} A nucleoside consists of a heterocyclic DNA base bound to a five-membered furanose ring (ribose or deoxyribose) by a glycosidic bond.⁸ Even a minor modification of the base or furanose ring can significantly affect the conformational structure and biological functions of the nucleoside. Modified nucleosides are used to create new pharmaceuticals.⁸ The presence of a glycosidic bond predetermines the lower thermal stability of nucleosides in comparison with DNA bases. Laser evaporation is generally used to transfer such thermostable molecules to an isolated state.^{6,7} We have shown previously that the classical matrix isolation spectroscopy method⁹ and the thermodynamically equilibrium process of evaporation from a Knudsen cell can be used to study nucleosides in isolated state.

As a structural DNA fragment, the thymidine nucleoside (Fig. 1) is a subject of numerous studies.^{10–13} The structure was mainly studied using polycrystalline samples, solutions, and quantum chemical computational methods.^{12,13} In the first experimental studies performed using the matrix isolation method,^{9,14} it was shown that *anti*- and *syn*- conformers of thymidine with various intramolecular hydrogen bonds were present in the matrices (O5'H...O2, O5'H...O3', O3'H...O5'). However, no detailed analysis of the population of thymidine conformers detected in the matrix was carried out. Nucleosides are known to have a very complex conformational structure in isolated state.¹³ For example, quantum chemical calculations using the DFT//B3LYP/6-31G(d,p) and MP2/6-311++G(d,p)//DFT//B3LYP/6-31G(d,p) methods show that thymidine has 92 stable conformers.¹³ There are 22 conformers in the relative energy range of 0–1.5 kcal/mol,¹³ and only some of them have clearly distinguishable characteristic bands. Specific features of matrix isolation spectroscopy allow even such

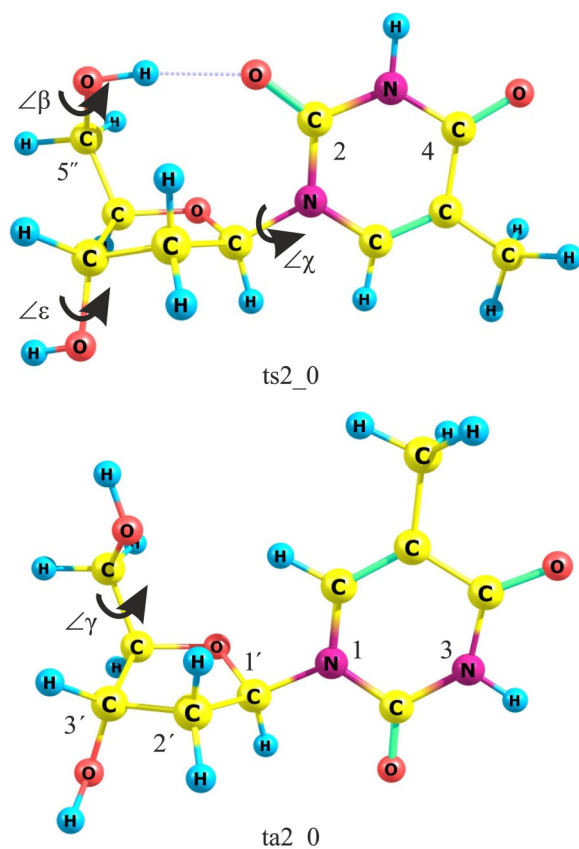


FIG. 1. Atomic numbering, torsion angles and structures of the main *syn*- (*ts2_0*) and *anti*- (*ta2_0*) conformational isomers of thymidine. The dotted line shows the intramolecular hydrogen bonds.

a complex system to be analyzed.¹⁵ When an impurity molecule is cooled in the matrix, some conformers can pass to lower-energy levels and the number of conformations decreases. Due to the high resolution of the matrix isolation method, it allows one to determine the absorption bands of OH and NH groups involved in the intramolecular hydrogen bonds that characterize the molecular structure of certain conformers. To determine the structure, the calculated and experimental vibrational spectra are compared. Using this scenario, we studied a number of pyrimidine and purine nucleosides (2'-deoxyuridine,^{15–17} uridine¹⁸ 2'-deoxyadenosine,¹⁹ and adenosine.²⁰ In this work, special attention was paid to the analysis of individual fragments of the potential energy surface and calculation of the height of barriers between the main thymidine conformers using the DFT/B3LYP and MP2 methods. To reach a more accurate interpretation of experimental infrared absorption spectra, the spectra of O5',O3',N3-deuteriothymidine molecules isolated in Ar matrices were also measured. The vibrational spectra of the main conformers were calculated not only by the DFT/B3LYP method in harmonic approximation but also with anharmonic correction.

II. EXPERIMENTAL AND CALCULATION METHODS

The low-temperature Fourier IR spectra were measured using the experimental setup described previously.^{14,21,22} In this study, Fourier IR spectra of isolated thymidine (Thy) and O5',O3',N3-deuteriothymidine (Thy_d3) molecules in Ar matrices were recorded with an apodized resolution of 0.4 cm^{-1} in the ranges of 450–2700 and 1400–4000 cm^{-1} . In addition, the IR Fourier spectra of thymine and 1-methylthymine molecules isolated in Ar matrices were recorded. The molecular fluxes of biomolecules and inert gases were measured using a low-temperature quartz microbalance.^{21,22} The evaporation system allowed us to obtain a molecular flow of Thy molecules with an intensity of 50–70 $\text{ng}/(\text{s}\cdot\text{cm}^2)$ at temperatures of 415–435 K. The purity of the inert gas (Ar) was no worse than 99.99%.

To obtain O5',O3',N3-deuteriothymidine (Thy_d3), thymidine was recrystallized in D₂O at temperatures no higher than 55 °C (in order to exclude thermal destruction processes).²³ A separate vacuum chamber with a zeolite pump cooled with liquid nitrogen was used to remove D₂O. The fraction of incompletely deuterated molecules did not exceed 15%.

Quantum chemical calculations were performed using the Gaussian16 programs²⁴ and Firefly programs (version 8.0)²⁵ that partially use the code of the GAMESS program (US).²⁶ Part of the calculations was carried out at a personal workstation and on the grid cluster of B. Verkin Institute for Low Temperature Physics and Engineering of the National Academy of Sciences of Ukraine. The calculations of the vibrational spectra in a harmonic approximation and with consideration for the anharmonicity of oscillations were performed by a supercomputer cluster at the University of Arizona. The vibrational spectra were calculated using the 6-311++G(df,pd) basis with a dimension of 743 basis functions. The dimensions of correlation-corrected bases²⁷ cc-pVDZ, aug-cc-pVDZ, aug-cc-pVTZ were 325, 551, and 1285 basis functions, respectively. The calculations were performed by density functional (DFT//B3LYP) and second-order Møller–Plesset perturbation theory methods (MP2). The standard capabilities of the GAMES program were used to estimate the relative free energies (ΔG) of conformers.

The torsion angles in the Thy molecule are shown in Fig. 1: C4'C5'O5'H ($\Delta\beta$), C3'C4'C5'O5' ($\Delta\gamma$), O4'C1'N1C2 ($\Delta\chi$), C4'C3'O3'H' ($\Delta\epsilon$). The designations of these angles and the method for calculating the pseudo rotation angle of the ribose ring (ΔP) comply with the Saenger's monograph.⁸ The conformations with *anti*-rotation of the pyrimidine ring around the glycosidic bond and with *syn*-rotation are denoted as *tan_x* and *tsn_x*, respectively. In these designations, *n* indicates a non-planar ribose conformation (2-C2'-endo or 3-C3'-endo) and *x* represents the numbers ordered by an increase in the relative energy of the conformers.

To estimate the intensity of absorption lines in experimental spectra, complex contours of spectral lines were approximated by Gaussian functions using the FITYK program.²⁸ The SYNSPEC program²⁹ was used to convert the calculated spectra to a superposition of Gaussian contours followed by comparison with the experimental spectra.

III. RESULTS AND DISCUSSION

Figure 2 shows the region of stretching vibrations of Thy molecules in an Ar matrix. The spectra of 2'-deoxyuridine (2_dU) and

1-methylthymine and thymine bases are provided for comparison. The spectrum of 1-methylthymine allows an unambiguous identification of the $\nu\text{N}_3\text{H}$ vibration. The spectrum of thymine is provided to control the thermal destruction. The thermal destruction of nucleosides can be detected by the appearance of narrow absorption bands of the corresponding base in the spectrum (after breakdown of the glycosidic bond). A comparison of the spectra of Thy and thymine shows (Fig. 2) that no thermal destruction was observed in our experiments with an evaporation temperature range of 415–435 K.

The conformational equilibrium of the gas phase can be preserved in a low-temperature matrix (or a supersonic beam) only provided that the barriers between the conformers are sufficiently high.¹⁵ Let us consider the possibility of a transition (interconversion) between the ts_2_0 and ta_2_0 conformers shown in Fig. 1. Figure 2 shows a good coincidence of the shapes and positions of the spectral bands of Thy and 2_dU. This suggests that the conformational compositions of these nucleosides in the matrix are similar. Using the potential energy surface map in the coordinates of the angles χ and β , it was previously shown that the transition barrier between the analogous 2-deoxyuridine conformers exceeds 4 kcal/mol.¹⁷ In this paper, this assessment was made by varying the χ angle in various directions. As shown in Fig. 3, the calculated barrier height between the ts_2_0 and ta_2_0 conformers exceeds 6 kcal/mol. Experiments show that annealing of matrix samples at 25–30 K does not significantly affect the intensity of the characteristic bands of thymidine. This agrees with the experimental data obtained by the matrix isolation method for small molecules^{30,31} that estimate the boundary value of the barrier as 2.5–3 kcal/mol for a temperature of 30 K. Hence, it can be concluded that, under the experimental conditions we used to create the sample, the

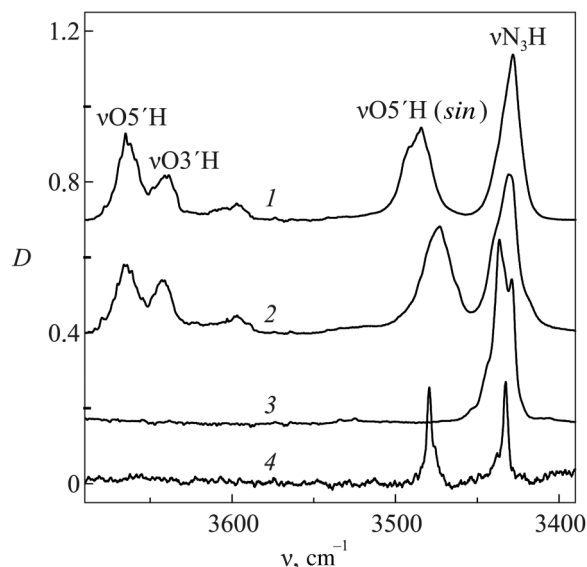


FIG. 2. The region of νOH , νNH stretching vibration of thymidine conformers (2), as well as 2'-deoxyuridine (1), 1-CH₃-thymine (3), and thymine (4) in an Ar matrix.

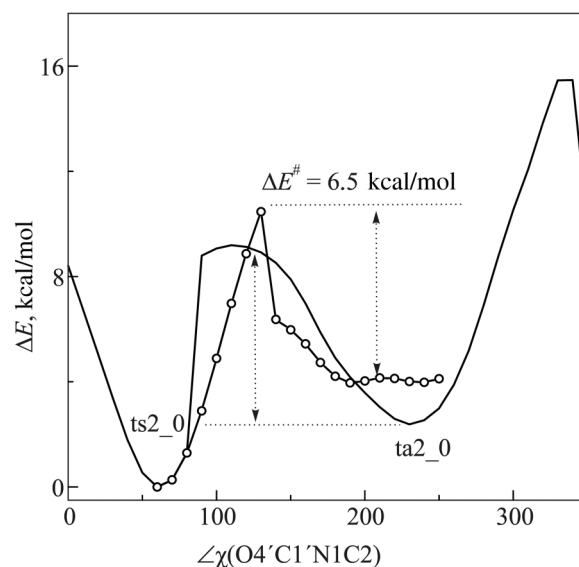


FIG. 3. The profile of the barrier of the *anti* → *syn* conformational transition in thymidine calculated by the DFT/B3LYP/cc-pvdz method with a step of 10° along the torsion angle χ . The circles indicate the profile of motion from *syn* (ts_2_0) to *anti* (ta_2_0).

interconversion between the thymidine *syn*- and *anti*-structures is completely absent.

However, the existence of low barriers is more likely within the *syn* and *anti* conformational families, since small fragments can rotate in them around angles $\angle\beta$, $\angle\gamma$ and $\angle\epsilon$, and also the angle of pseudo rotation of the ribose ring ($\angle\phi$) can change (Fig. 1). It was previously shown^{16,17} that low-barrier conformers of nucleosides are fixed in low-temperature matrices more poorly than conformers of small molecules. For example, the *syn*-conformer of 2'-deoxyuridine with C3'-endo structure of the sugar ring (the barrier of transition to C2'-endo is 1.3 kcal/mol¹⁶) is not preserved upon freezing in Ar and Kr matrices even at 6 K. Moreover, transition of the O3'H hydroxy group of 2'-deoxyuridine molecules through a 1.2 kcal/mol barrier was observed upon deposition into a Kr matrix at 6 K.¹⁷ Approximate estimates of the interconversion time show that in order to fix low-barrier conformers, the cooling time should be comparable to the period of phonon oscillations of the matrix and low-frequency vibrational modes of molecules.¹⁴ The effect of the matrix on the energy relaxation in impurity molecules was already observed experimentally.³¹ It can be assumed that the energy relaxation ("cooling") rates of individual vibrational modes in complex molecules will differ. In fact, unlike 2'-deoxyuridine, a uridine *syn*-conformer with a C3'-endo sugar ring structure and a barrier height of 2.1 kcal/mol was fixed in an Ar matrix, and its interconversion was only observed upon annealing to 30 K. Therefore, the minimum barrier height that ensures the fixation of low-barrier nucleoside conformers in Ar and Kr matrices can be estimated as 2 kcal/mol.

Figure 4(a) shows that the height of the barrier between the *anti*-conformers with the C2'-endo (ta_2_0) and C3'-endo (ta_3_0) sugar ring structures exceeds 2 kcal/mol, hence these

conformational families can be fixed in matrices. At the same time, the barrier height between the *syn*-conformers $ts2_0$ and $ts3_0$ is smaller than 1.5 kcal/mol [Fig. 4(b)].

The experimental spectra contain no characteristic absorption bands of $ts3_0$ near $3520\text{--}3530\text{ cm}^{-1}$ (Fig. 2). Therefore, we can assume that conformer $ts3_0$ passes into $ts2_0$ upon thymidine freezing in the matrix. This agrees with the results obtained for similar *syn*-structures of 2'-deoxyuridine in Ar and Kr matrices.¹⁶

The conformational pattern within each $ta2$ and $ta3$ family is determined by the rotations of the hydroxymethyl group ($\angle\gamma$) and hydroxy groups $O5'H$ ($\angle\beta$) and $O3'H$ ($\angle\epsilon$). Figure 5(a) shows a fragment of the potential energy surface for the $ta2$ family that has the shape of three ravines stretched along the abscissa axis ($\angle\beta$). The ravines are separated by high barriers. Inside each ravine there is only one minimum that can be fixed in the matrix [Fig. 5(b)]. The $ta2_0$ conformation is the global minimum of this family and has two low-barrier satellites ($< 0.5\text{ kcal/mol}$) that will pass to $ta2_0$ upon cooling in the matrix. The conformations of $ta2_1$, $ta2_2$ (Fig. 5) and their satellites are significantly lower in

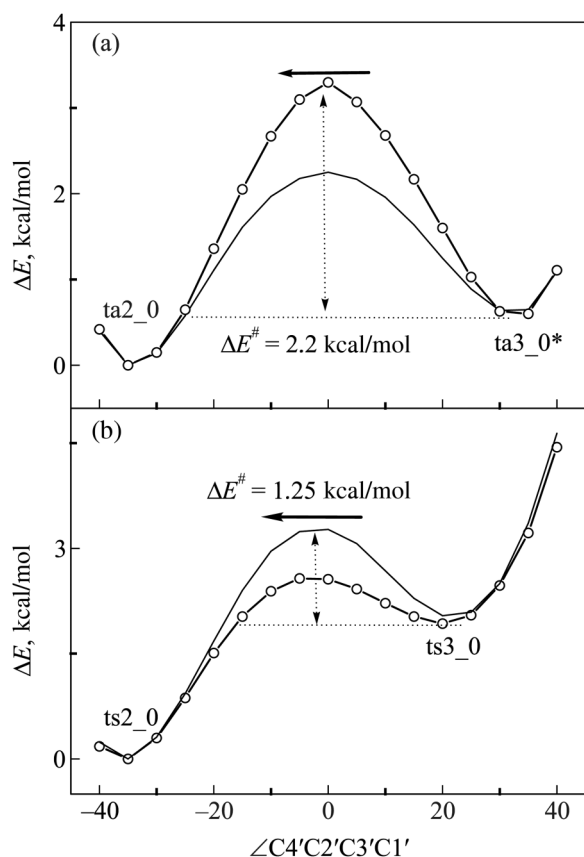


FIG. 4. Profiles of the barriers of C3'-endo \leftrightarrow C2'-endo conformational transitions for the main *anti*- (a) and *syn*-conformers (b) of thymidine. The calculations were performed using the DFT/B3LYP/cc-pvdz (line) and MP2/cc-pvdz (circles) methods.

energy than $ta2_0$ ($> 2\text{ kcal/mol}$) and have no well-defined characteristic bands.

The potential energy surface of the *anti*-conformer family with C3'-endo structure of the deoxyribose ring is shown in Fig. 6(a). The $ta3_0$ conformation is the global minimum of this family. Unlike the $ta2_0$ conformer, the low-barrier satellites of $ta3_0$ are much closer in energy to the global minimum [Fig. 6(b)]. Though the energy of the $ta3_0$ conformation is lower, the $ta3_1$ and $ta3_2$ structures are interesting for further consideration. Like in the case of 2'-deoxyuridine,¹⁵⁻¹⁷ these conformations are characterized by intramolecular hydrogen bonds $O5'H\cdots O3'H$ and $O3'H\cdots O5'H$. The weak absorption band near 3600 cm^{-1} in the spectrum can correspond to these bonds (Fig. 2).

There are no clearly defined extended ravines on the surface maps of the potential energy of thymidine *syn*-conformers plotted as functions of β and γ angles (Fig. 7). The $ts2_0$ conformation is the global minimum of the family of *syn*-conformers with the C2'-endo structure of the deoxyribose ring [Fig. 7(a)]. Obviously, it has no satellites caused by rotation of the $O5'H$ hydroxy group ($\angle\beta$). The low-barrier satellite of this conformation is $ts3_0$, the global minimum of the *syn*-conformer family with the C3'-endo structure of the deoxyribose ring [Fig. 7(b)]. The $ts2_1$ structure on the surface map of this family is of interest. A specific feature of this structure is that the hydrogen atom of the $O5'H$ hydroxy group can interact with $O4'$, perhaps through a very weak intramolecular hydrogen bond. As a result, the absorption band of the stretching vibrations of $\nu O5'H$ can shift to the $3620\text{--}3640\text{ cm}^{-1}$ region. However, the stability of this structure during deposition into a matrix is not guaranteed. The $ts3_1$ and $ts3_2$ structures [Fig. 7(b)] are *syn*-analogues of minor *anti*-conformations $ta3_1$ and $ta3_2$ with $O5'H\cdots O3'$ and $O3'H\cdots O5'$ intramolecular hydrogen bonds, respectively. However, they are inferior in energy to these conformations, therefore they are not discussed below in detail.

The $ta2_0$, $ta3_0$, and $ts2_0$ conformations possess not only the low-barrier structural satellites discussed above (Figs. 4-7). Additional conformational structures can be formed by rotation of the $O3'H$ hydroxy group that is reflected by angle $\angle\epsilon$. The profiles of barriers of conformational transitions formed by this rotation are shown in Fig. 8. One can see that each basic conformation ($ta2_0$, $ta3_0$, $ts2_0$) has one low-barrier satellite which is certainly unstable upon deposition into a matrix. Moreover, each basic conformation has one structure with a 1.55-1.6 kcal/mol barrier (Fig. 8). Given this barrier height, it is difficult to accurately predict the behavior of a conformer upon deposition into a matrix. These satellite structures have no well-defined characteristic bands, therefore more detailed calculations were not carried out for these structures. For the $ta2_0$ [Fig. 8(b)] and $ta3_0$ [Fig. 8(c)] conformations, the angle $\angle\epsilon$ is close to 180° . For $ts2_0$, two almost identical minima can be seen [Fig. 8(a)]. The $ts2_0$ structure with the $\angle\epsilon$ angle of 300° [Fig. 8(a)] was chosen based on additional calculations by the MP2/aug-cc-pVDZ method.

Based on the analysis made, six basic conformations of thymidine were selected for more accurate calculations of relative energies (using the MP2 method) and vibrational spectra (Table 1). Although the $ts3_0$ conformer passes into the $ts2_0$ structure, these calculations were performed for it as well in order to determine more accurately the population of $ts2_0$ in low-temperature

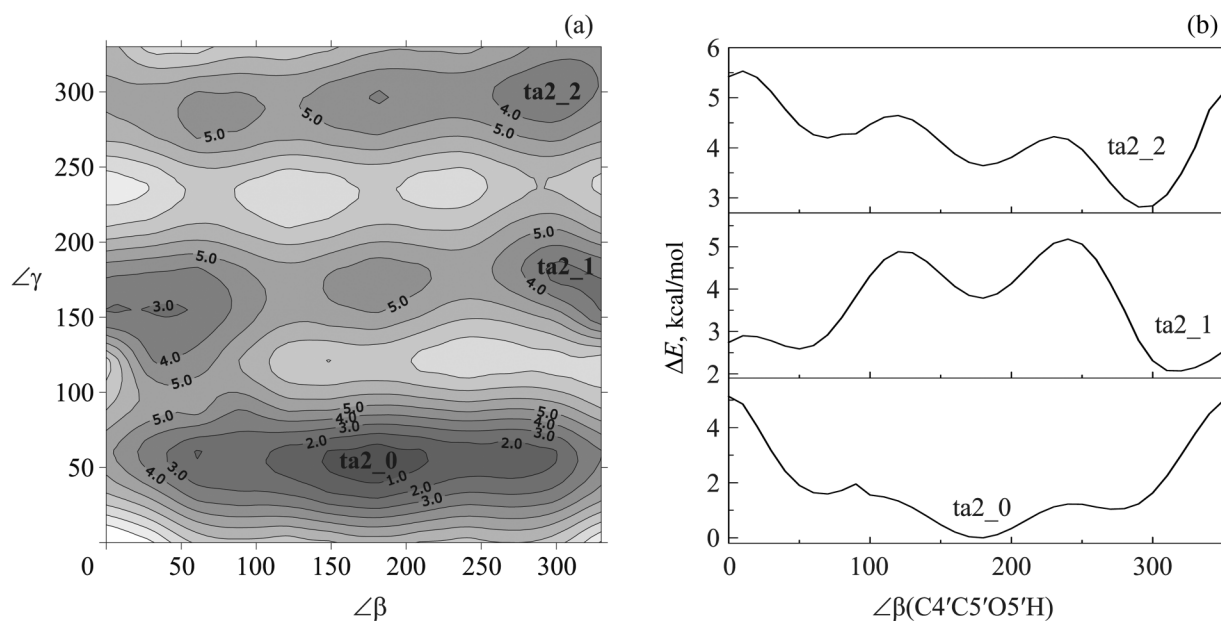


FIG. 5. The surface map of the potential energy of thymidine *anti*-conformers with the C2'-endo structure of the deoxyribose ring. The calculation of the surface (a) and the profile of ravines (b) was performed using the DFT/B3LYP/cc-pVDZ method. The surface isolines are marked in kcal/mol.

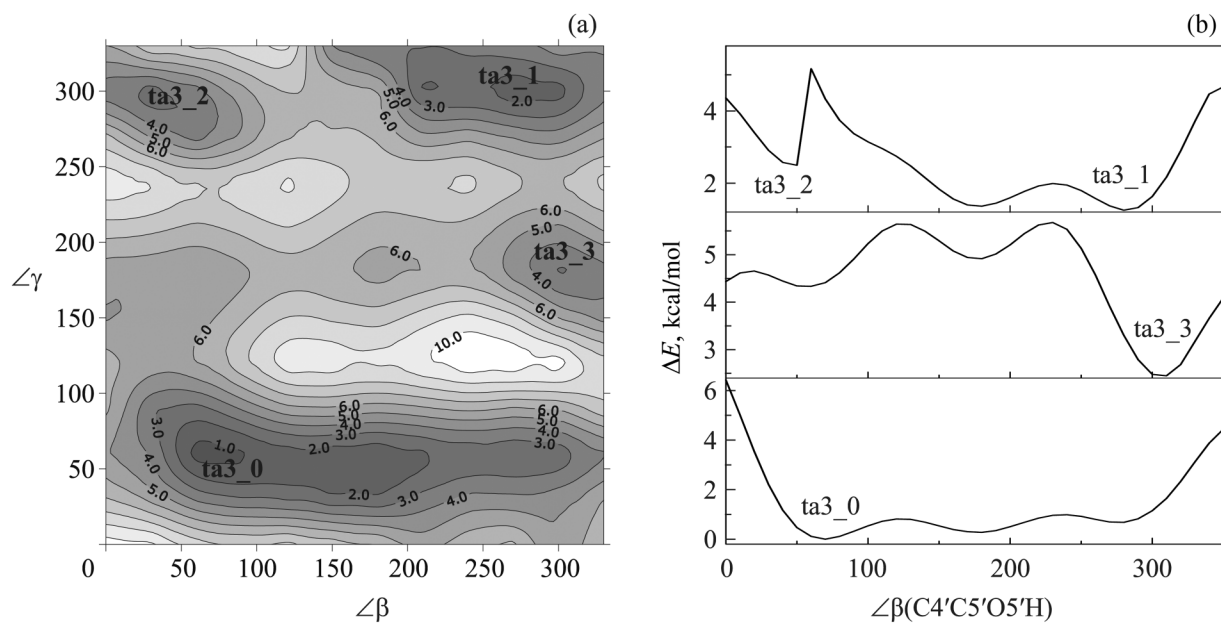


FIG. 6. The surface map of the potential energy of thymidine *anti*-conformers with the C3'-endo structure of the deoxyribose ring. The calculation of the surface (a) and the profile of ravines (b) was performed using the DFT/B3LYP/cc-pVDZ method. The surface isolines are marked in kcal/mol.

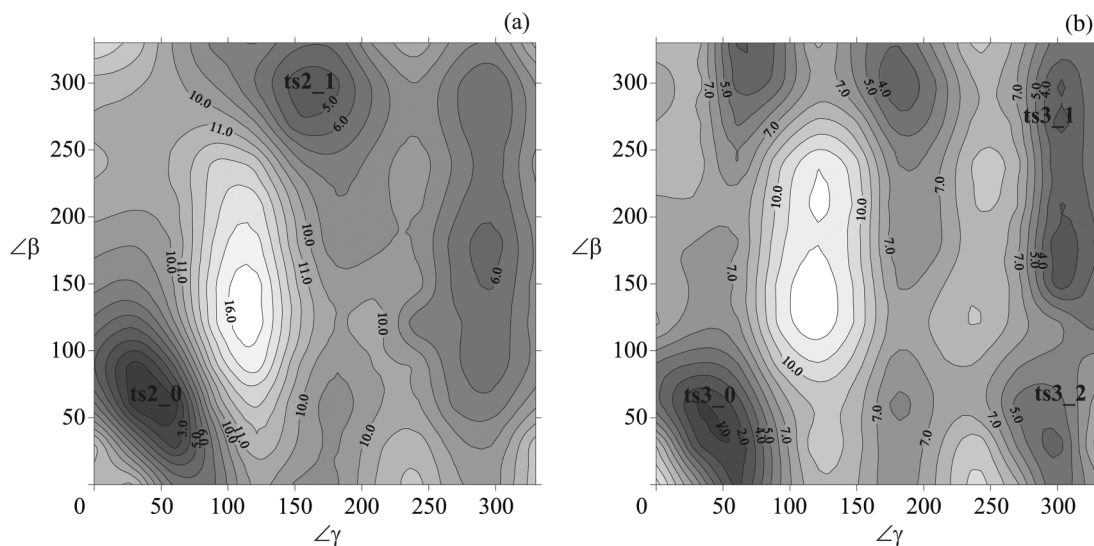


FIG. 7. The surface map of potential energy of thymidine *syn*-conformers with the O2'H...O2 intramolecular hydrogen bond and conformations of the deoxyribose ring: C2'-endo (a), C3'-endo (b). The surface isolines are marked in kcal/mol.

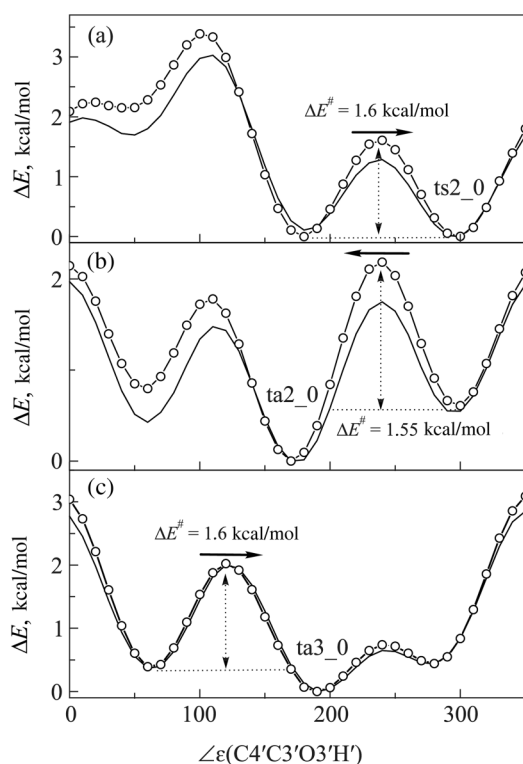


FIG. 8. The profiles of barriers of conformational transitions formed upon rotation of the O3'H group for various *syn* and *anti* thymidine conformers. Calculations by the DFT/B3LYP/cc-pvdz (line) and MP2/cc-pvdz (circles) methods.

matrices. With the same purpose, DFT calculations were performed for a number of structural satellites of the main conformers. The results of energy calculations presented in Table I show that the ts2_0 conformer is the most stable structure, regardless of the calculation method. However, taking into account the corrections for the Gibbs free energy at the evaporation temperature used in the experiment (420 K), it follows that the free energy global minimum corresponds to the ta3_0 conformer (Table I). To calculate the populations of conformers in the gas phase, the following formula was used³²:

$$N_j(T) = \frac{k_j e^{-\Delta G_j(T)/RT}}{\sum_{i=0}^n k_i e^{-\Delta G_i(T)/RT}} 100\%, \quad (1)$$

where k_j is the coefficient of degeneration of conformation j .

The populations were calculated taking 7 low-barrier satellites (Figs. 5–8) for each *anti*-conformation (ta2_0 and ta3_0) and 4 satellites for the *syn*-conformation (ts2_0) into account. In order to take the population of *syn*-analogs of ta3_1 and ta3_2 conformations into account (Figs. 6 and 7) without complicating the analysis, it was assumed that these conformations are twice degenerate. As a result, calculations by Eq. (1) predict a noticeable dominance of *anti*-conformations in the matrix samples (Table I). The calculated values of ΔG and, accordingly, the occupancies can be checked using the equation that partially uses experimental data:

$$\begin{aligned} \Delta G_{AB}(T) &= -RT \ln K_{AB} \\ &= -RT \ln (I_{A,E} I_{B,C} / I_{A,C} I_{B,E}), \end{aligned} \quad (2)$$

where $I_{A,E}$, $I_{B,E}$ are the experimental intensities of characteristic bands of conformers A and B; $I_{A,C}$ and $I_{B,C}$ are the calculated intensities presented in Table II.

TABLE I. Structural parameters (characteristic angles) and relative energies (ΔE , ΔG in kcal/mol) of the basic thymidine conformers.

Torsion angles	Conformers					
	ta2_0	ta3_0	ta3_1	ta3_2	ts3_0	ts2_0
$\angle P$	166	25	25	22	39	166
$\angle \chi$	-129	-133	-163	-166	60	62
$\angle \gamma$	52	65	-58	-69	43	44
$\angle \beta$	177	72	178	42	42	64
$\angle \varepsilon$	174	-167	-55	-86	-86	-65
Energies and calculation method						
ΔE DFT/cc-pvdz	2.1	2.8	3.8	4.6	1.9	(-875.20662) 0
ΔE DFT/aug-cc-pvdz	1.67	2.01	2.30	4.0	1.59	(-875.28237) 0
ΔE MP2/aug-cc-pvdz	1.81	2.46	3.66	4.63	1.99	(-872.92318) 0
ΔE MP2/aug-cc-pvtz	2.19	2.71				(-873.66672) 0
ΔG (420 K) aug-cc-pVDZ ^a	0.32 ^a	0.0 ^a	1.24	2.14	0.84	0.04
Matrix population,% (calculation)	26.2	38.8	4.9	1.7		28.4
Matrix population,% (calculation + experiment)	29	43	6	2	-	20

^aAveraged ΔE values calculated by the MP2/aug-cc-pvdz and MP2/aug-cc-pvtz methods.

TABLE II. Experimental frequencies (cm^{-1}) and intensities of the absorption bands in the range of stretching vibrations νOH , $\nu\text{NH}\nu\text{CO}$, νC5C6 of Thy (Thy_d3) molecules in Ar matrices, as well as the vibration frequencies and intensities of the main Thy (Thy_d3) conformers calculated by the DFT/B3LYP/6-311++G(df,pd) method.

Vibration	Conformer												
	ta2_0		ta3_0		ta3_1		ta3_2		ts2_0		Ar matrix		
	ν , cm^{-1}	I_c	ν , cm^{-1}	I_c	ν , cm^{-1}	I_c	ν , cm^{-1}	I_c	ν , cm^{-1}	I_c	ν , cm^{-1}	I_c	
$\nu\text{O5}'\text{H}$	3662	47	3636	34	3669	60					3665	3.3	
	3670 ^a		3644 ^a										
	(2704)	30	(2683)	34	(2709)	40					(2704)	1.1	
$\nu\text{O3}'\text{H}$	3643	36	3663	53			3646	46	3645	35	3642	2.0	
	3653 ^a		3672 ^a						3656 ^a				
	2789	24	(2704)	22			(2692)	30	(2691)	23	(2688)	0.7	
νO3H - hydrogen bond with $\text{O5}'$					3598	91					3597	0.5	
					(2656)	54					(2656)	0.2	
νO5H - hydrogen bond with $\text{O2}'$							3596	71					
							(2655)	44					
νO5H - hydrogen bond with N3									3489	3478 ^a	488	3474	6.5
									(2578)	(2572) ^a	259	(2569)	2.5
νN3H	3429	66.5	3426	70.6	3426	70.3	3426	68.7	3422	70.5	3430	7.5	
	3436 ^a		3430 ^a						3429 ^a		(2552,		
	(2548)	44	(2546)	47	(2546)	46	(2546)	45	(2543)	45	2533)	0.9	
νC2O	1730	561	1736	558	1737	563	1723	384	1724	291	1727	34	
	1736 ^a		1736 ^a						1729 ^a				
	(1726)	423	(1733)	425	(1734)	429	(1721)	318	(1723)	266	(1729)	10	
νC4O	1711	824	1716	803	1715	805	1712	981	1712	1257	1714	51	
	1713 ^a		1725 ^a						1714 ^a				
	(1698)	971	(1703)	942	(1703)	946	(1697)	1055	(1696)	1312	(1703)	16	
$\nu(\text{C5} = \text{C6})$	1657	66	1658	64	1659	68	1646	64	1656	56	1662	2	
	1654 ^a		1656 ^a						1655 ^a				
	(1657)	53	(1658)	53	(1658)	56	(1646)	53	(1656)	41	(1665)	1.6	

Note: I_c is the calculated intensities, km/mol; I_e is the integral experimental intensities. The calculated vibration frequencies νOH , νNH were multiplied by a correction factor of 0.95168 (0.96434 for νOD , νND Thy_d3); the νCO , νC5C6 vibration frequencies were multiplied by 0.978. The numbers in parenthesis is the Thy_d3 frequencies.

^aAnharmonic frequencies based on the anharmonic problem solution using the vibrational second-order perturbation theory (VPT2).

The absorption band of the experimental spectrum with a maximum at 3664 cm^{-1} represents the superposition of the absorption bands of the most populated *anti*-conformers $ta2_0$, $ta3_0$, and $ta3_1$ (Table II). This allows one to adjust the total population of the *syn*- and *anti*-subsets of conformers using Eq. (2). The averaged intensity of the O5'H vibration band equal to 50 km/mol was chosen to perform the correction.

As a result, the population values obtained matched rather well the data obtained solely by calculations (Table I).

Based on the data of the population of conformers in the matrix, it can be seen that the majority of bands in the experimental spectrum belongs to the $ta3_0$, $ta2_0$, and $ts2_0$ conformations. Therefore, Table II presents the calculated characteristics of the absorption bands of the stretching vibrations of the OH, NH, and CO groups in these conformations. In the range of νOH , νNH stretching vibrations, a DFT/B3LYP/6-311++G(df,pd) calculation in harmonic approximation shows a good agreement between the calculated and experimental frequencies if the correction factor ("scaling factor") of 0.95168 is used (Table II). The calculated spectrum of thymidine is also in good agreement with the experimental spectrum [Fig. 9(a)]. The calculated spectrum was visualized for superposing the absorption bands of oscillations of the 5 main conformers with consideration for their population (Table I). To visualize the calculated absorption band, a half-width of the Gauss contour equal to 10 cm^{-1} was chosen. This choice is due to the fact that the vibrational bands of non-planar molecules in the matrix can broaden significantly.²¹ Comparison of the experiment and calculations shows that the greatest deviation from the experiment is demonstrated by the absorption band of the hydrogen-bonded $\nu\text{O5}'\text{H}$ vibration in the $ts2_0$ conformer. An increase in the absorption frequency of this vibration by 15 cm^{-1} is observed [Table II, Fig. 9(a)]. This frequency shift can occur due to the effect of the matrix on the anharmonicity of this vibration. It is interesting to note that the DFT/B3LYP/6-311++G(df,pd) calculation based on the anharmonic problem solution using the vibrational second-order perturbation theory (VPT2) implemented in the GAUSSIAN16 program significantly reduces the frequency mismatch for this vibration (Table II). Moreover, the frequencies of the absorption bands of other νOH and νNH vibrations calculated using VPT2 can be compared with the experiment without applying the "scaling factor" (Table II).

In the spectrum of Thy_d3, the absorption bands of the νOD and νND vibrations shift to $2700\text{--}2500\text{ cm}^{-1}$ and their intensities decrease markedly [Fig. 9(b)]. The results of spectral calculations by the DFT/B3LYP/6-311++G(df,pd) method in a harmonic approximation and with correction by a factor of 0.96434 well agree with the experimental spectrum [Fig. 9(b) and Table II]. This is observed for all the spectral bands in this range, except for the νN3D vibration band [Fig. 9(b)]. The absorption band of this vibration overlaps with the $\nu\text{O5}'\text{D}$ band of the $ts2_0$ conformer [Fig. 9(b)] and is split into two bands with frequencies of 2552 and 2533 cm^{-1} [Fig. 9(b) and Table II]. The frequencies of these two bands are shifted in different directions from the calculated frequency of 2543 cm^{-1} of νN3D vibrations [Fig. 9(b) and Table II]. This splitting may result from the Fermi resonance. It is facilitated by the fact that, in comparison with νN3H , the νN3D vibration frequency is shifted to the $2500\text{--}2800\text{ cm}^{-1}$ range where a few variants

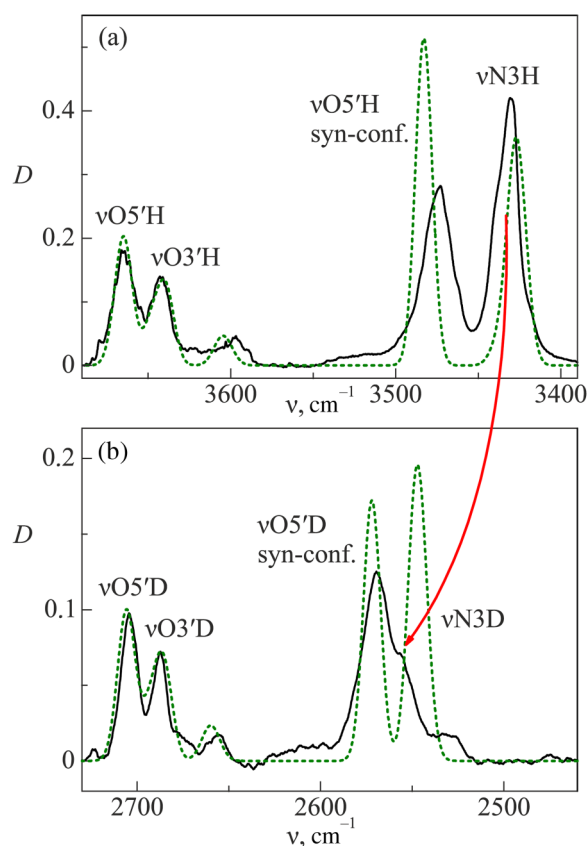


FIG. 9. The region of stretching vibrations (νNH , νOH) of thymidine (a) and (νND , νOD) of deuteriothymidine (b) in Ar matrices. The dotted line shows a visualization of the calculated spectrum.

of combinational bands are possible.³³ Previously, we have already detected a splitting of the νN3D vibration band for deuterated 5I-uracil caused by the Fermi resonance.³³

Calculations show that the frequencies of νCO stretching vibrations insignificantly differ from each other (Table II). Therefore, the νCO , νC2O and νC4O νCO in the synthesized calculated spectrum are well separated [Fig. 10(a)]. However, nearly a single broad absorption band is observed in the experimental spectrum [Fig. 10(a)]. This broadening of the absorption bands of νCO vibrations can also be caused by the Fermi resonance that often manifests itself in this region of the spectrum of pyrimidine bases.²¹ In particular, the Fermi resonance produces 5 additional absorption bands in the spectrum of 1-methylthymine near the absorption bands of νCO fundamental vibrations [Fig. 10(a)]. The results of anharmonic calculations by the VPT2 method also indicate the possibility of the Fermi resonance in this spectral region. According to the calculations for νC2O and νC4O vibrations of $ta2_0$ and $ta3_0$ conformers, the Fermi resonance with several Raman modes is possible. These modes are formed by bending vibrations of the pyrimidine ring whose frequencies lie in the ranges of $1100\text{--}1295$ and $480\text{--}650\text{ cm}^{-1}$.

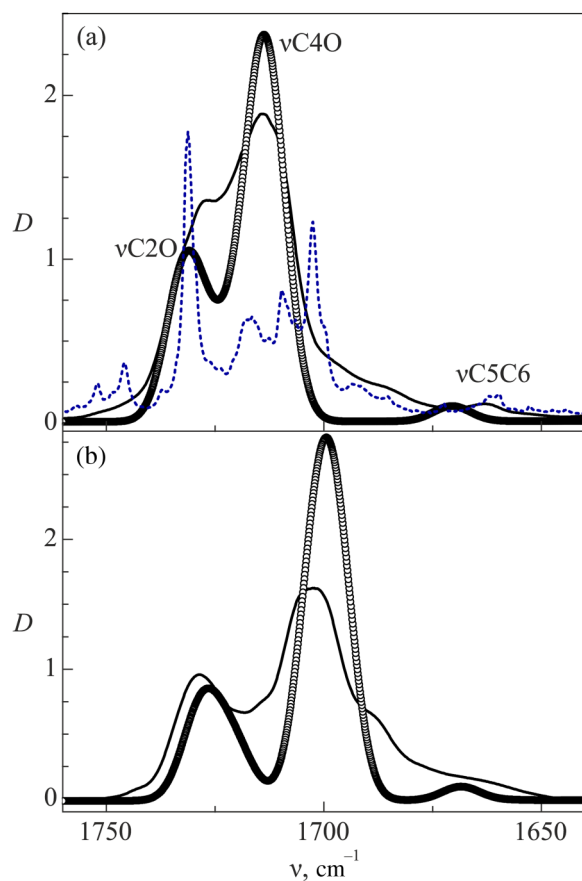


FIG. 10. The region of stretching vibrations of the CO group (ν CO) for thymidine, 1-methylthymine (a) and trideuteriothymidine (b) in Ar matrices. The spectrum of 1-methylthymine is shown by a dotted line. The line composed of circles shows a visualization of the calculated spectra of nucleosides.

Deuteration can significantly change the resonance conditions, both due to the effect of certain vibrations on anharmonicity and due to a significant shift in the frequencies of combination vibration bands. The experimental spectrum of Thy_d3 manifests a distinct separation of absorption bands of the ν C2O and ν C4O vibrations and hence a good agreement between the experimental and calculated spectra [Fig. 10(b)].

IV. CONCLUSION

Using IR Fourier spectroscopy of molecules in inert matrices and quantum-mechanical calculations, it has been shown that the equilibrium in the gas phase between the main *anti*- and *syn*-conformers of thymidine is preserved upon freezing in inert Ar matrices. The overall populations of *anti*- and *syn*-conformers in inert Ar matrices at temperatures of 6–11 K are ca. 80 and 20%, respectively.

Two *anti*-conformers of thymidine differing in the structures of the deoxyribose ring: C2'-endo and C3'-endo, dominate. These

conformers have several structural satellites with low barriers that can completely pass into the main structures when thymidine molecules enter the matrix. Owing to the interconversion of satellite structures, the population of *anti*-conformers with a C3'-endo deoxyribose ring in the matrix can significantly exceed the population of similar C2'-endo structures.

The C2'-endo conformation of the deoxyribose ring is predominant for *syn*-conformers. The fact that the population of *anti*-conformers in the ts2_0 *syn*-conformer is lower can be explained by the smaller number of low-barrier satellite conformations.

The spectra of deuteriothymidine show an overlapping of the ν N3D vibration bands and the stretching vibration of the O5'D group of deoxyribose that is linked by an intramolecular hydrogen bond to the C2O group of the pyrimidine base ring. This is facilitated by the splitting of the ν N3D absorption band (2543 cm^{-1}) due to the Fermi resonance with the Raman modes of the pyrimidine ring.

This study was supported by the National Academy of Sciences of Ukraine (grants No. 0117U002287, No. 07-01-18, and No. 15/19H). The authors are grateful to A.M. Plokhotnichenko for helpful advice in discussing the work. The calculations were performed at the computer center of the B. Verkin Institute for Low Temperature Physics and Engineering of the National Academy of Sciences of Ukraine and the University of Arizona computer center to which the authors are grateful for the computing resources provided.

REFERENCES

- ¹Nucleic acid in the Gas Phase, edited by V. Gabelica (Springer-Verlag, Berlin, Heidelberg, 2014).
- ²M. S. de Vries and P. Hobza, *Annu. Rev. Phys. Chem.* **58**, 585 (2007).
- ³R. Weinkauff, J.-P. Schermann, M. S. de Vries, and K. Kleinermanns, *Eur. Phys. J. D* **20**, 309 (2002).
- ⁴R. N. Casaes, J. B. Paul, R. P. McLaughlin, R. J. Saykally, and T. van Mourik, *J. Phys. Chem. A* **108**, 10989 (2004).
- ⁵J. P. Simons, R. A. Jockusch, P. Carcabal, I. H. Nig, R. T. Kroemer, N. A. MacLeod, and L. C. Snoek, *Int. Rev. Phys. Chem.* **24**, 489 (2005).
- ⁶R. Wu, B. Yang, G. Berden, J. Oomens, and M. T. Rodgers, *J. Phys. Chem. B* **119**, 2795 (2015).
- ⁷J.-Y. Salpin and D. Scuderi, *Rapid Communications in Mass Spectrometry* **29**, 1898 (2015).
- ⁸W. Saenger, *Principles of Nucleic Acids Structure* (Springer-Verlag, New York, 1984).
- ⁹S. A. Krasnokutski, A. Yu. Ivanov, V. Izvekov, G. G. Sheina, and Yu. P. Blagoi, *J. Mol. Struct.* **482–483**, 249 (1998).
- ¹⁰M. Tsuboi, M. Komatsu, J. Hoshi, E. Kawashima, T. Sekine, Y. Ishido, M. P. Russell, J. M. Benevides, and G. J. Thomas, Jr., *J. Am. Chem. Soc.* **119**, 2025 (1997).
- ¹¹S. Ptasinska, P. Candori, S. Denifl, S. Yoon, V. Grill, P. Scheier, and T. D. Mark, *Chem. Phys. Lett.* **409**, 270 (2005).
- ¹²A. Hocquet, N. Leulliot, and M. Ghomi, *J. Phys. Chem. B* **104**, 4560 (2000).
- ¹³Y. P. Yurenko, R. O. Zhurakivsky, M. Ghomi, S. P. Samijlenko, and D. M. Hovorun, *J. Phys. Chem. B* **111**, 9655 (2007).
- ¹⁴A. Yu. Ivanov, S. A. Krasnokutski, and G. G. Sheina, *Fiz. Nizk. Temp.* **29**, 1065 (2003) [*Low Temp. Phys.* **29**, 809 (2003)].
- ¹⁵A. Yu. Ivanov, S. A. Krasnokutski, G. Sheina, and B. Yu.P., *Spectrochim. Acta A* **59**, 1959 (2003).
- ¹⁶A. Yu. Ivanov and V. A. Karachevtsev, *Fiz. Nizk. Temp.* **33**, 772 (2007) [*Low Temp. Phys.* **33**, 590 (2007)].
- ¹⁷A. Yu. Ivanov, *Fiz. Nizk. Temp.* **34**, 962 (2008) [*Low Temp. Phys.* **34**, 762 (2008)].
- ¹⁸A. Yu. Ivanov, *Fiz. Nizk. Temp.* **36**, 571 (2010) [*Low Temp. Phys.* **36**, 458 (2010)].

- ¹⁹A. Yu. Ivanov, *Fiz. Nizk. Temp.* **40**, 727 (2014) [*Low Temp. Phys.* **40**, 565 (2014)].
- ²⁰A. Yu. Ivanov, Y. V. Rubin, S. A. Egupov, L. F. Belous, and V. A. Karachevtsev, *Fiz. Nizk. Temp.* **41**, 1198 (2015) [*Low Temp. Phys.* **41**, 936 (2015)].
- ²¹A. Yu. Ivanov, A. M. Plokhotnichenko, E. D. Radchenko, G. G. Sheina, and Yu. P. Blagoi, *J. Mol. Struct.* **372**, 91 (1995).
- ²²A. Yu. Ivanov and A. M. Plokhotnichenko, *Instr. Experim. Techn.* **52**, 308 (2009).
- ²³J. M. Gavira, M. Campos, G. Diaz, A. Hernanz, and R. Navarro, *Vibrational Spectroscopy* **15**, 1 (1997).
- ²⁴M. J. Frisch, G. W. Trucks, H. B. Schlegel, G. E. Scuseria, M. A. Robb, J. R. Cheeseman, G. Scalmani, V. Barone, G. A. Petersson, H. Nakatsuji, X. Li, M. Caricato, A. V. Marenich, J. Bloino, B. G. Janesko, R. Gomperts, B. Mennucci, H. P. Hratchian, J. V. Ortiz, A. F. Izmaylov, J. L. Sonnenberg, D. Williams-Young, F. Ding, F. Lipparini, F. Egidi, J. Goings, B. Peng, A. Petrone, T. Henderson, D. Ranasinghe, V. G. Zakrzewski, J. Gao, N. Rega, G. Zheng, W. Liang, M. Hada, M. Ehara, K. Toyota, R. Fukuda, J. Hasegawa, M. Ishida, T. Nakajima, Y. Honda, O. Kitao, H. Nakai, T. Vreven, K. Throssell, J.A. Montgomery, Jr., J.E. Peralta, F. Ogliaro, M. J. Bearpark, J. J. Heyd, E. N. Brothers, K. N. Kudin, V. N. Staroverov, T. A. Keith, R. Kobayashi, J. Normand, K. Raghavachari, A. P. Rendell, J. C. Burant, S. S. Iyengar, J. Tomasi, M. Cossi, J. M. Millam, M. Klene, C. Adamo, R. Cammi, J. W. Ochterski, R. L. Martin, K. Morokuma, O. Farkas, J. B. Foresman, and D. J. Fox, *Gaussian 16, Revision B.01* (Gaussian, Inc., Wallingford, CT, 2016).
- ²⁵Ae A. Granovsky, *Firefly Version 7.1.G* (2009).
- ²⁶M. W. Schmidt, K. K. Baldrige, J. A. Boatz, S. T. Elbert, M. S. Gordon, J. H. Jensen, S. Koseki, N. Matsunaga, K. A. Nguyen S. Su, T. L. Windus, M. Dupuis, and J. A. Montgomery, *J. Comput. Chem.* **14**, 1347 (1993).
- ²⁷T. H. Dunning, Jr., *J. Chem. Phys.* **90**, 1007 (1989).
- ²⁸M. Wojdyr, *J. Appl. Cryst.* **43**, 1126 (2010).
- ²⁹K. Irikura, *Program SYNOPSIS* (National Institute of Standards and Technology, Gaithersburg, MD, USA, 1995).
- ³⁰A. J. Barnes, *J. Mol. Struct.* **113**, 161 (1984).
- ³¹I. D. Reva, S. G. Stepanian, L. Adamowicz, and R. Fausto, *Chem. Phys. Lett.* **374**, 631 (2003).
- ³²J. H. Jensen and M. S. Gordon, *J. Am. Chem. Soc.* **113**, 7917 (1991).
- ³³A.Yu. Ivanov, Yu.V. Rubin, S.A. Egupov, L. F. Belous, V. A. Karachevtsev, *Fiz. Nizk. Temp.* **40**, 1409 (2014) [*Low Temp. Phys.* **40**, 1097 (2014)].

Translated by [AIP Author Services](#)